Electronic Supplementary Material (ESI) for Journal of Materials Chemistry A.
This journal is © The Royal Society of Chemistry 2020

Supplemental Information

Impact of Particle Size on Kinetics and Structure Stability of Single-Crystal Li-rich Cathode Materials

Jianming Sun[a, d], Xin Cao[c,*], Wuhai Yang[a, d], Eunjoo Yoo[a, d,*] and Haoshen Zhou[a, b, d,*]

Affiliations:

[a]Energy Technology Research Institute, National Institute of Advanced Industrial Science and Technology (AIST), 1-1-1, Umezono, Tsukuba 305-8568, Japan

[b]Center of Energy Storage Materials & Technology, College of Engineering and Applied Sciences, Jiangsu Key Laboratory of Artificial Functional Materials, National Laboratory of Solid State Microstructures, and Collaborative Innovation Center of Advanced Microstructures, Nanjing University, Nanjing 210093, P. R. China

[c]Jiangsu Key Laboratory of New Power Batteries, Jiangsu Collaborative Innovation Center of Biomedical Functional Materials, School of Chemistry and Materials Science, Nanjing Normal University, Nanjing 210023, PR China

[d]Graduate School of System and Information Engineering, University of Tsukuba, 1-1-1, Tennoudai, Tsukuba 305-8573, Japan

*Correspondence to: xincao@njnu.edu.cn (Xin Cao), yu.eunjoo@aist.go.jp (Eunjoo Yoo), hszhou@nju.edu.cn (Haoshen Zhou)

EXPERIMENTAL PROCEDURES

Synthesis of Single-Crystal $Li_{1.2}Ni_{0.2}Mn_{0.6}O_2$

Single-crystal $Li_{1.2}Ni_{0.2}Mn_{0.6}O_2$ was synthesized by the co-precipitation-assisted molten salt method. The co-precipitation method was used to prepare the hydroxide precursor of materials. The stoichiometric $NiSO_4 \cdot 6H_2O$ and $MnSO_4 \cdot 7H_2O$ were dissolved in a mixture of deionized water for 2 mol/L SO_4^{2-} concentration. Then, the mixture solution of 4 mol/L NaOH solution and 4 mol/L $NH_3 \cdot H_2O$ was added into the above mixture with $NiSO_4 \cdot$and $MnSO_4$. After the co-precipitation reactions, the $Ni_{0.25}Mn_{0.75}(OH)_2$ precipitant as precursor was washed, dried, and collected. The dark yellow precursor was mixed with Li_2CO_3 as lithium source and LiCl as molten salt, which had a weight ratio of precursor + Li_2CO_3/LiCl = 1 : 3, and next calcined at 900 °C for 9, 10, 11, and 12 h in air. After high temperature reaction, the product was washed using deionized water to remove excess Li salts. the samples prepared at different calcination times are denoted as SCL-9h, SCL-10h, SCL-11h, and SCL-12h.

Materials characterization

The structure of the SCL-9h, SCL-10h, SCL-11h, and SCL-12h samples were identified by X-ray Powder Diffraction (XRD, Ultima III, Rigaku Corporation) radiation from Cu Kα (λ = 1.5406 Å). The data were collected between diffraction angles (2θ) from 10° to 80° at the scan rate of 2° per min. Rietveld refinements of the XRD pattern obtained by GSAS2+EXPGUI suite. The morphologies of the materials were procured by Scanning Electron Microscope (SEM, JSM-7000F). Raman spectra of the materials were obtained using a homemade mold and JASCO microscope spectrometer (NRS-1000DT). Transmission Electron Microscope (TEM) and High Resolution Transmission Electron Microscope (HR-TEM) images were taken with a JEM-200c transmission electron microscope operated at 200 kV. Software Image J with particle size statistic function was used to examine the grain sizes.

Galvanostatic Intermittent Titration Technique (GITT):

To reveal the mechanism, GITT was tested to find out the kinetics Li+ diffusion coefficient (D_{Li^+}) of SCL-9h, SCL-10h, SCL-11h, and SCL-12h samples. The D_{Li^+} can be determined by inducing Fick's second law of diffusion based on some reasonable assumptions. Thus, the equation can be simplified to

$$D_{Li^+} = \frac{4}{\pi\tau}\left(\frac{n_m V_m}{S}\right)^2\left(\frac{\Delta E_s}{\Delta E_t}\right)^2 \quad \text{(S1)}$$

where τ is the limited time, nm is the mole number of the electrode, Vm is the molar volume of the $Li_{1.2}Ni_{0.2}Mn_{0.6}O_2$, S is the area of the electrode, ΔEs and ΔEt are the change in the steady state potential and the total change during the current flux by deducting the IR drop [S1, S2]. The cell was performed at the current density of 0.1 C with a voltage window from 2 to 4.8 V and tested 2 h with current flux followed by 5 h rest to reach the quasi-equilibrium potential, which was repeated until the end.

Electrochemical measurement:

2032 coin-type cells were used for electrochemical measurements for half cells. The SCL-9h, SCL-10h, SCL-11h, and SCL-12h samples as electrodes have consisted of active material, Super P, and polyvinylidene difluoride (PVDF) binder with the weight ratio of 70:20:10. The mass loading of the four cathode materials in this work were controlled in a range of 0.8 ± 0.1 mg/cm^2 in the of half coin cells. The 1 mol/L $LiPF_6$ in EC/DEC were prepared as the electrolyte, and a glass fiber film was employed as the separator. The testing coin-type cells were assembled in an argon-filled glovebox. The galvanostatic charge-discharge tests were performed by using a Hokuto Denko HJ1001SD8 battery tester at different conditions. Electrochemical impedance spectroscopy (EIS) data and cyclic voltammetry (CV) data were performed with the frequency range and amplitude from 10 mHz to 100 kHz and 10mV, respectively.

For the full cell, the mass loading of the four cathode materials in this work were controlled in a range of 0.8 ± 0.1 mg/cm^2 in the of half coin cells. The capacity ratio of the Si/C anode and cathode (N/P) were controlled to be around 1.1−1.2. Before assembling to the full cell, the graphite anode needed to be prelithiated. The Si/C materials were purchased from BTR New Materials Group Co. LTD, China. The Si/C materials as anodes have consisted of active material, Super P, and carboxymethyl cellulose (CMC) binder with the weight ratio of 75:15:10. 1 mol/L LiPF6 in EC/DEC were prepared as the electrolyte, and a glass fiber film was employed as the separator. During the prelithiated process, the Si/C electrode was assembled to the half-cell with metal Li for three cycles and got discharged. Then, this half-cell was disassembled. The Si/C electrode was picked out from it carefully and washed by the electrolyte in the coin-type cell. The testing coin-type cells were assembled in an argon-filled glovebox.

For the pouch Li-rich||Si/C full cell, the electrodes, electrolyte and separator were exactly the same as the coin-type full cell. The prelithiated Si/C electrode was picked out from the half pouch cell for three cycles, and then it was thermally sealed in the Al plastic film with the single-layer Li-rich cathode (30 × 40 mm) and glass-fiber separator in an argon-filled glovebox. The galvanostatic charge-discharge tests were performed by using a Hokuto Denko HJ1001SD8 battery tester at different conditions.

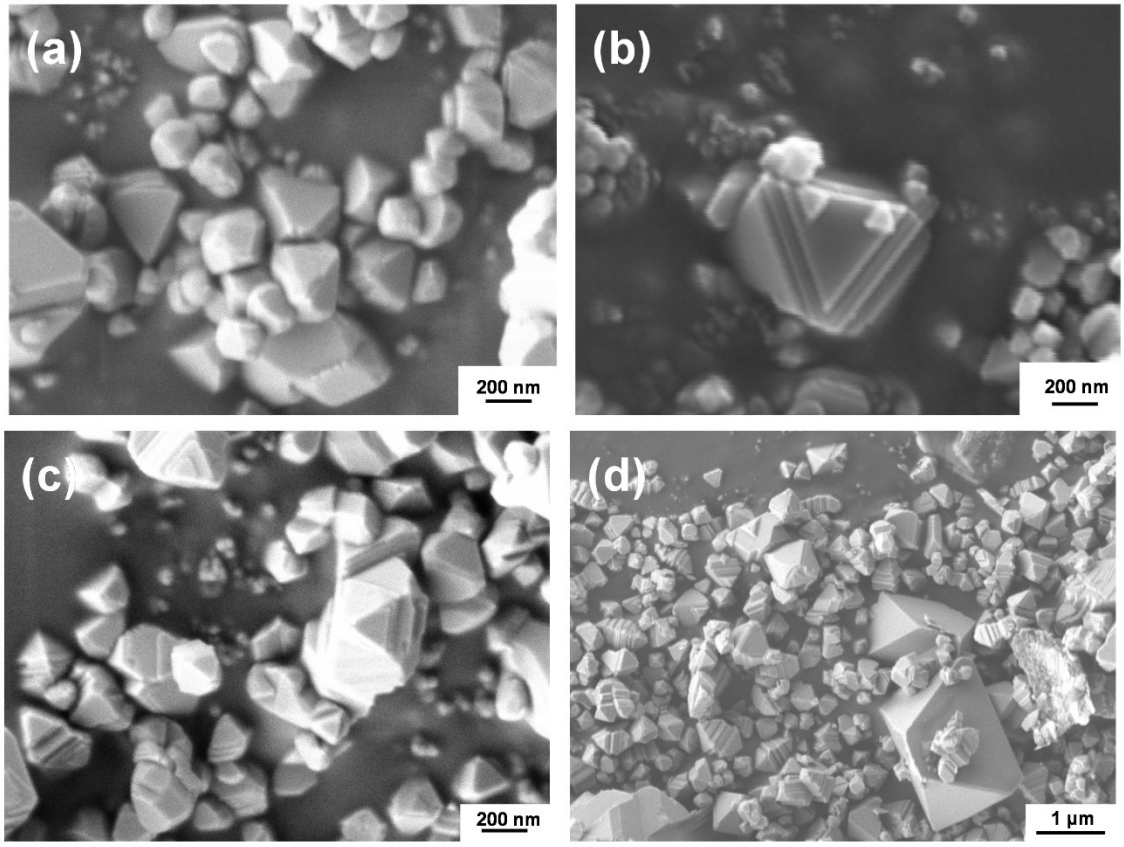

Figure S1. SEM images of (a) SCL-9h, (b) SCL-10h, (c) SCL-11h, and (d) SCL-12h samples.

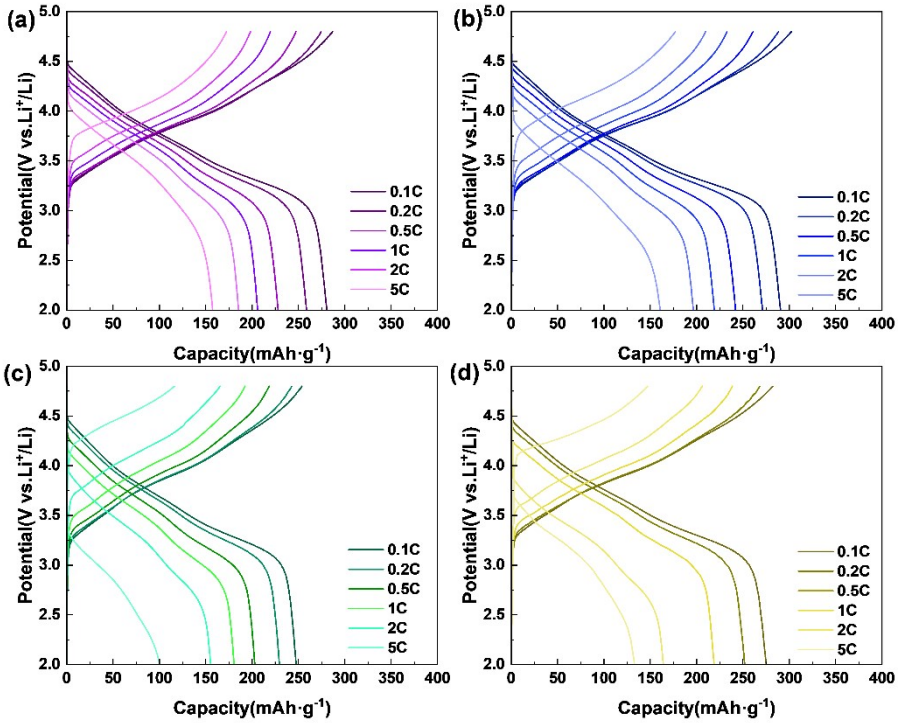

Figure S2. Charge-discharge curves of the (a) SCL-9h, (b) SCL-10h, (c) SCL-11h, and (d) SCL-12h samples at the different current densities of 0.1, 0.2, 0.5, 1, 2, and 5 C.

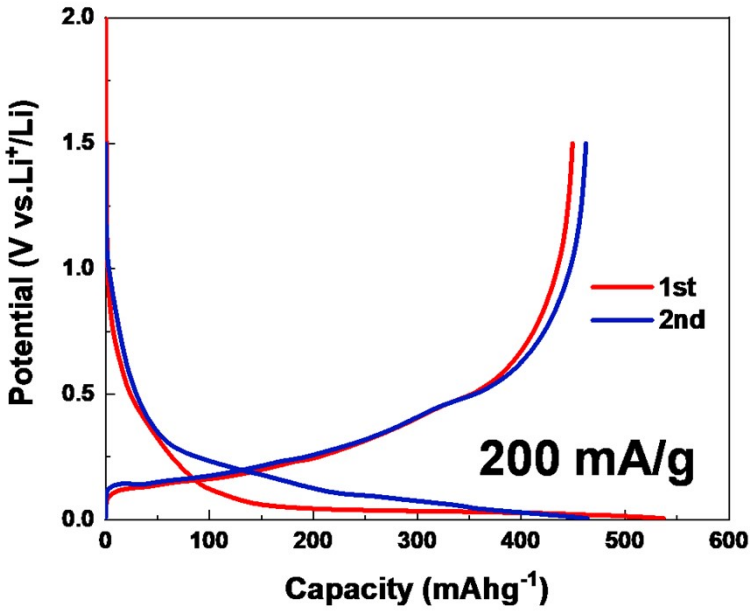

Figure S3. Charge-discharge curves of the Si/C anode material (vs. Li) at the current densities of 200 mA/g.

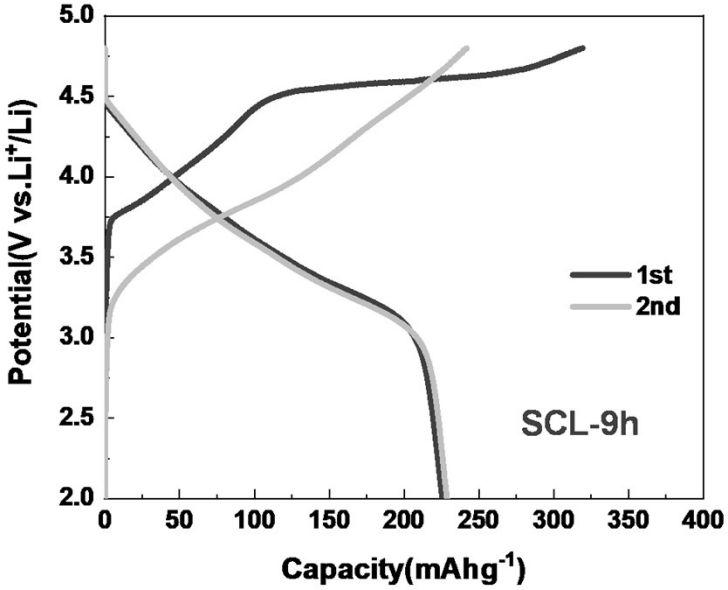

Figure S4. The charging and discharging curves of SCL-9h cathodes during the initial two cycles in the voltage window of 2.0−4.8 V at the current density of 0.1 C in the full pouch cell (vs. Si/C anode).

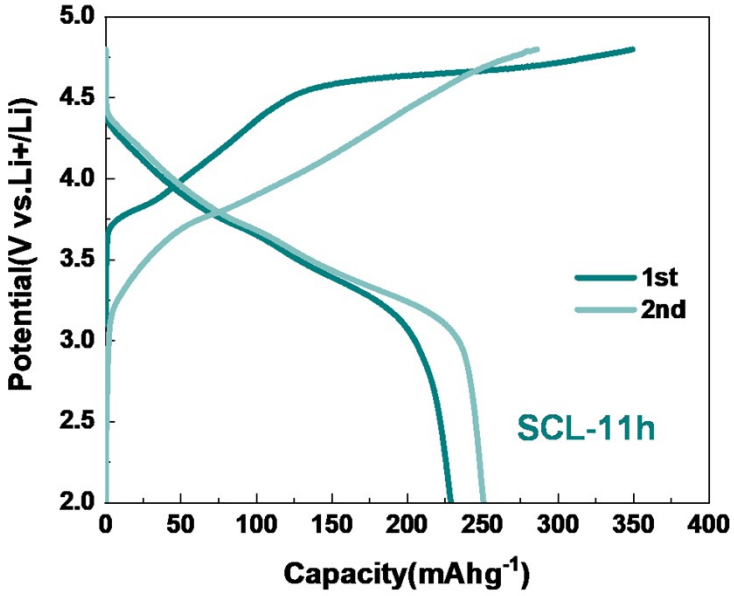

Figure S5. The charging and discharging curves of SCL-11h cathodes during the initial two cycles in the voltage window of 2.0−4.8 V at the current density of 0.1 C in the full pouch cell (vs. Si/C anode).

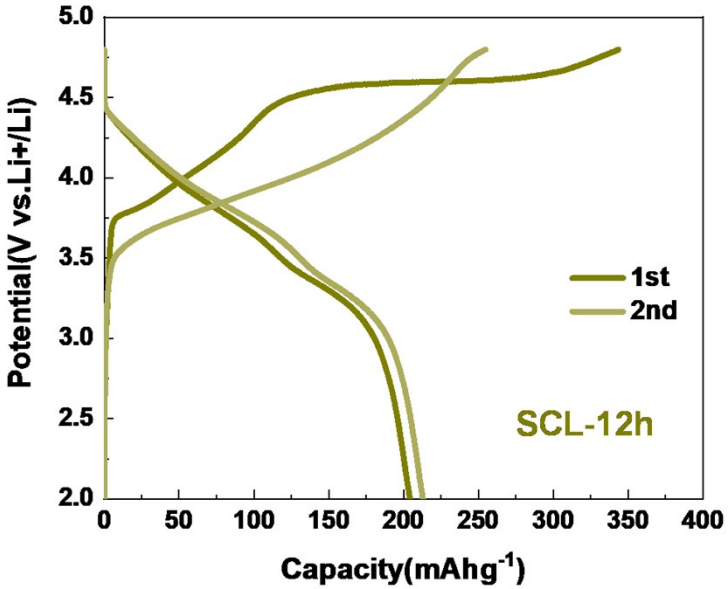

Figure S6. The charging and discharging curves of SCL-12h cathodes during the initial two cycles in the voltage window of 2.0−4.8 V at the current density of 0.1 C in the full pouch cell (vs. Si/C anode).

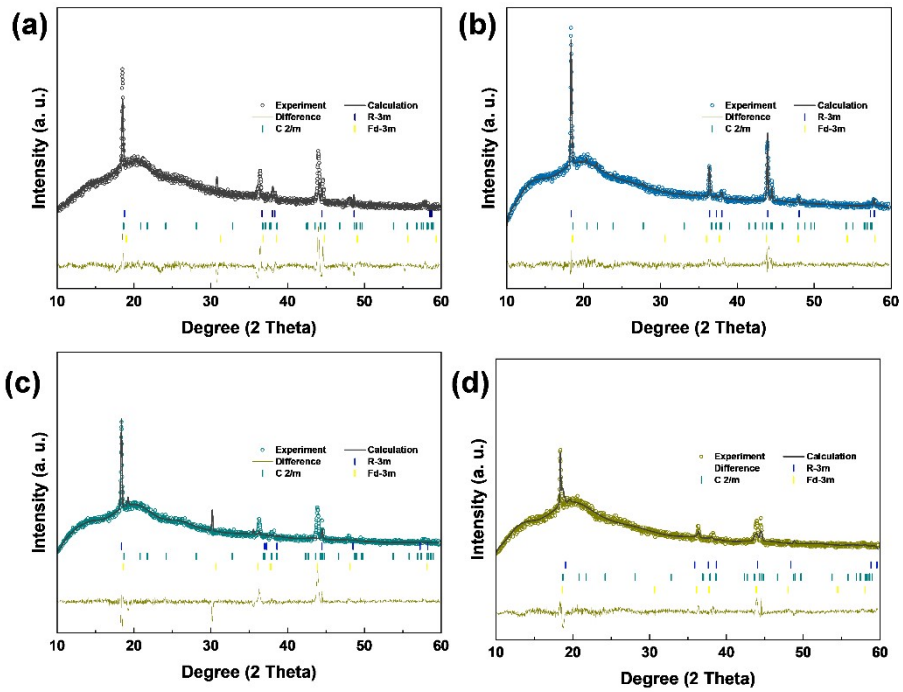

Figure S7. The XRD Rietveld refinement results of (a) SCL-9h, (b) SCL-10h, (c) SCL-11h, and (d) SCL-12h samples after 250 cycles.

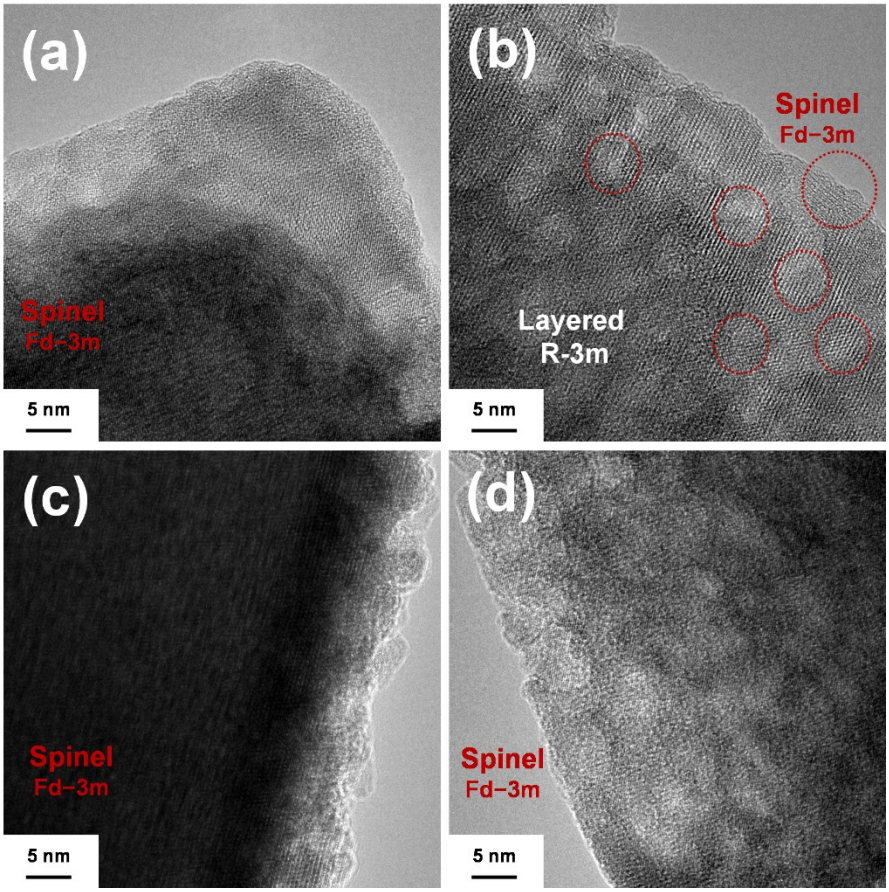

Figure S8. The HR-TEM images of (a) SCL-9h, (b) SCL-10h, (c) SCL-11h, and (d) SCL-12h samples after 250 cycles.

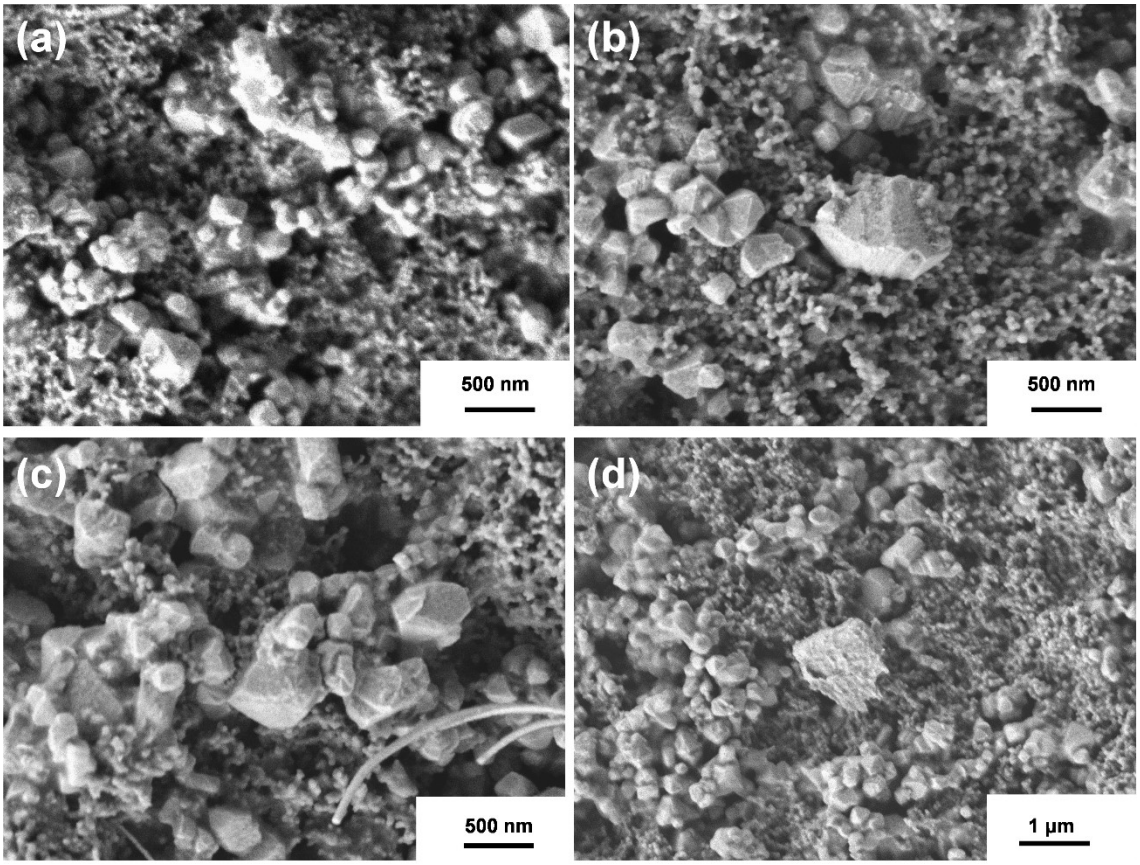

Figure S9. The SEM images of (a) SCL-9h, (b) SCL-10h, (c) SCL-11h, and (d) SCL-12h samples after 250 cycles.

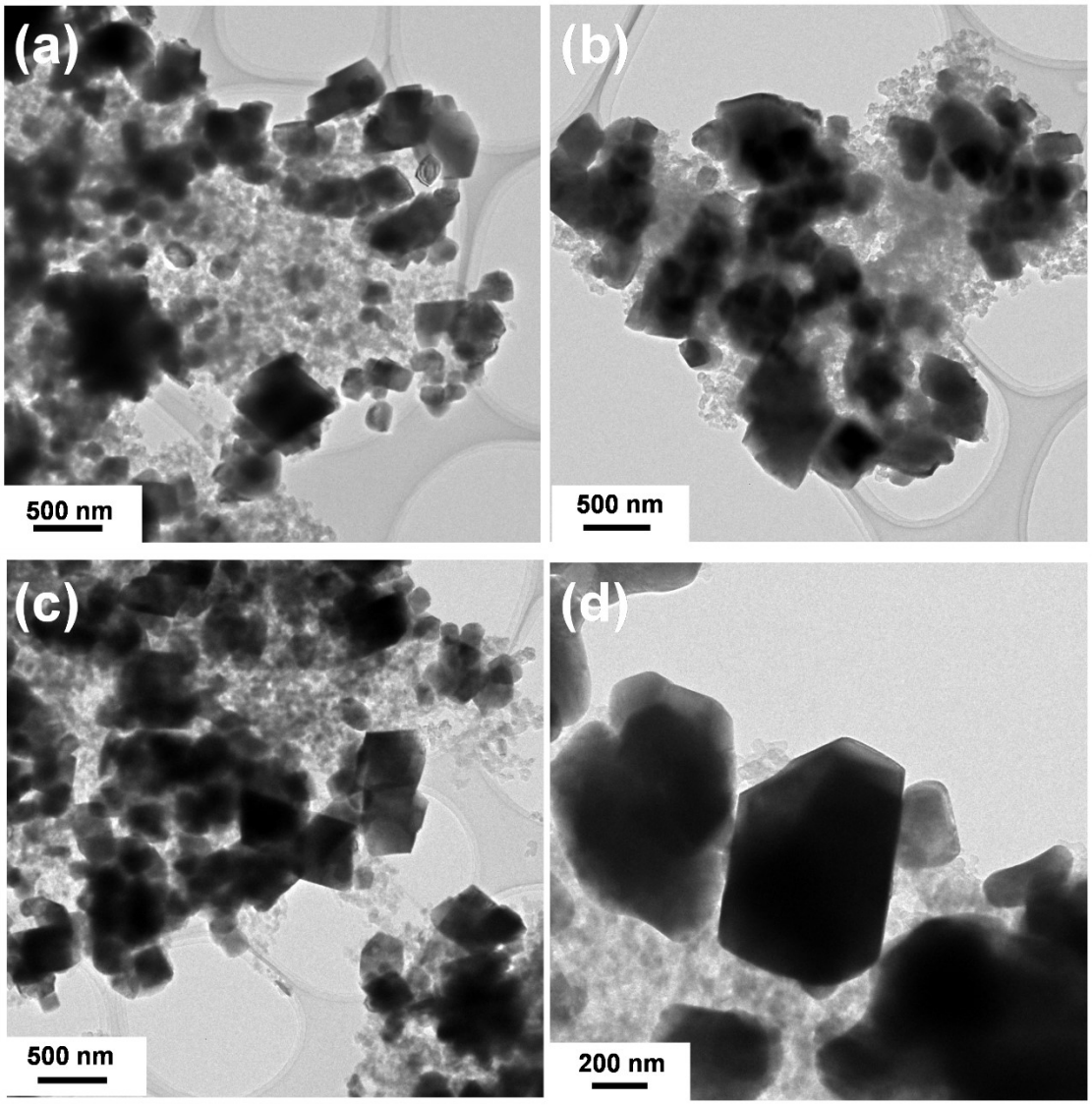

Figure S10. The TEM images of (a) SCL-9h, (b) SCL-10h, (c) SCL-11h, and (d) SCL-12h samples after 250 cycles.

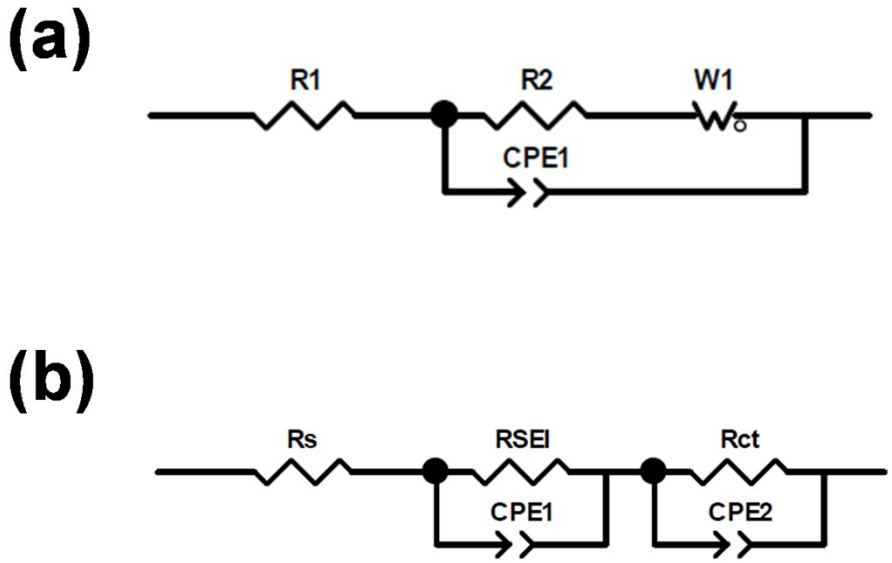

Figure S11. The TEM images of (a) SCL-9h, (b) SCL-10h, (c) SCL-11h, and (d) SCL-12h samples after 250 cycles.

Table S1. Crystallographic parameters were obtained from the Rietveld refinement for SCL-9h, SCL-10h, SCL-11h, and SCL-12h samples.

Refined parameters		Sample			
		SCL-9h	**SCL-10h**	**SCL-11h**	**SCL-12h**
R-3m $\alpha = \beta = \gamma = 90°$	a, b (Å)	2.86470(14)	2.8678(5)	2.86582(9)	2.86599(13)
	c (Å)	14.2486(4)	14.2963(5)	14.2792(12)	14.2539(7)
	V ($Å^3$)	101.265(8)	101.829	101.562(10)	101.394(8)
C2/m $\alpha = \gamma = 90°$,	a (Å)	4.9786(18)	4.9732(7)	4.9670(12)	4.883(11)
	b (Å)	8.5792(32)	8.5609(5)	8.5755(20)	8.492(19)
	c (Å)	5.0408(14)	5.0606(8)	5.0396(7)	5.036(7)
	β(°)	109.34(4)	109.719	109.557(14)	106.02(15)
	V($Å^3$)	203.15(13)	202.829	202.28(8)	200.7(7)
R_{wp}/χ^2		5.33%/1.26	2.13%/1.32	3.15/1.96	4.32/1.85

Table S2. Crystallographic parameters were obtained from the Rietveld refinement for SCL-9h, SCL-10h, SCL-11h, and SCL-12h samples after cycles.

Refined parameters		Sample			
		SCL-9h	**SCL-10h**	**SCL-11h**	**SCL-12h**
R-3m α = β = 90° γ = 120°	a, b (Å)	2.89064(22)	2.87293(33)	2.87252(7)	2.86524(3)
	c (Å)	14.4536(33)	14.3464(32)	14.2792(6)	14.2539(5)
	V ($Å^3$)	104.591(27)	102.548(28)	101.562(2)	101.394(3)
C2/m α = γ = 90°,	a (Å)	4.9368(0)	5.0010(21)	4.9690(9)	4.883(7)
	b (Å)	8.5316(0)	8.607(4)	8.586 (1)	8.487(7)
	c (Å)	5.0302(0)	5.0746(17)	5.0401(0)	5.036(2)
	β (°)	109.451(0)	109.783(24)	109.554(1)	106.021(1)
	V ($Å^3$)	199.770(0)	205.55(15)	202.35(7)	201.9(6)
Fd-3m α = β = γ = 90°	a, b, c (Å)	8.224(6)	8.2164(30)	8.2682(4)	8.228(2)
	V ($Å^3$)	556.3(7)	554.7(4)	565.248(0)	558.583(3)
R_{wp}/χ^2		9.64%/5.25	4.55%/1.96	9.13%/5.22	4.79%/2.12

Table S3. Data from the EIS Fitting Curves of SCL-9h, SCL-10h, SCL-11h, and SCL-12h samples at the pristine state.

Sample	R_s (Ω)	R_{ct} (Ω)
SCL-9h	2.491	475.8
SCL-10h	2.013	250.7
SCL-11h	2.789	283.1
SCL-12h	3.324	404.6

Table S4. Data from the EIS Fitting Curves of SCL-9h, SCL-10h, SCL-11h, and SCL-12h samples after cycles.

Sample	R_s (Ω)	R_{ct} (Ω)	R_{SEI} (Ω)
SCL-9h	3.655	117.2	1516
SCL-10h	3.044	198.6	2771
SCL-11h	2.651	254.9	2189
SCL-12h	2.743	246.3	1459

References

[S1] T. Wu, X. Zhang, Y. Wang, N. Zhang, H. Li, Y. Guan, D. Xiao, S. Liu, H. Yu, *Adv. Funct. Mater.* 2023, **33**, 2210154.

[S2] Y. Zhang, C. Yin, B. Qiu, G. Chen, Y. Shang, Z. Liu, *Energy Stor. Mater.,* 2022, **53**, 763.